

AFOSR-TN-57-540

ASTIA Document No. AD 136 526

ENGINEERING RESEARCH INSTITUTE
THE UNIVERSITY OF MICHIGAN
ANN ARBOR

AN INVESTIGATION OF REACTIONS IN FERROSPINELS
BY DIFFERENTIAL THERMAL ANALYSIS

Technical Report No. 4
Solid State Devices Laboratory
Department of Electrical Engineering

C. F. Jefferson

Project 2495

AIR FORCE OFFICE OF SCIENTIFIC RESEARCH
AIR RESEARCH AND DEVELOPMENT COMMAND
SOLID STATE SCIENCE DIVISION
CONTRACT NO. AF 18(603)-8, DIVISION FILE NO. 40-24

July 1957

ABSTRACT

Differential thermal analysis has been used to follow the oxidation of magnetite in solid solution with a nickel-zinc ferrospinel, and the solid-state reaction leading to the formation of the ferrospinel from the oxides. Differential thermal curves for the series $\text{Ni}_{.474}\text{Zn}_{.526}\text{Fe}_2\text{O}_4 - \text{Fe}_3\text{O}_4$ are shown and explained. An attempt was made to follow the solid-state reaction which occurs during the formation of the ferrospinel from the oxides.

THE OXIDATION OF THE SYSTEM $\text{Ni}_{.474}\text{Zn}_{.526}\text{Fe}_2\text{O}_4 - \text{Fe}_3\text{O}_4$

Ferros spinels utilized as ferromagnetic elements in electric circuits have the advantages of high permeability combined with high resistivity. One detrimental factor which contributes to the lowering of the resistivity is ferrous iron in the structure. Ferrous iron also effects the anisotropy and magnetostriction which in turn effect the permeability. It is therefore necessary to understand the conditions under which it forms and methods of oxidizing it once it has formed, to control better the magnetic properties of the ferros spinels.

The usual procedure for the preparation of the nickel-zinc ferrite is to mix intimately NiO , ZnO , and Fe_2O_3 in the desired proportions, press them into the required form, and fire at 1100°C to 1400°C until the solid-state reaction has been completed. Ferrous iron will form if Fe_2O_3 is present in excess of the amount required for the formation of $\text{Ni}_x\text{Zn}_{1-x}\text{Fe}_2\text{O}_4$. Jefferson¹ has investigated the formation of ferrous iron in a nickel zinc ferros spinel under these conditions. When the oxides are mixed in stoichiometric proportions, there are two mechanisms by which ferrous iron can form. The formation below about 1300°C is caused by localized nonstoichiometric regions. Ferrous iron content due to this cause can be minimized by thorough mixing of the oxides and a prolonged firing time. The effect of firing time and extent of mixing on ferrous iron formation in a stoichiometric nickel-zinc ferros spinel was investigated and reported by Jefferson and Grimes.² Above about 1300°C , the presence of ferrous iron in stoichiometric material is due to the decomposition of the nickel-zinc ferros spinel. Van Uitert³ has shown that volatilization of zinc occurs, which leaves the material with an excess of Fe_2O_3 . Ferrous iron formation by this mechanism increases with firing, rather than decreases as occurs in the first case.

It has been known for some time that two iron sesquioxides exist. $\alpha\text{Fe}_2\text{O}_3$ is the common form and has the hexagonal structure. $\gamma\text{Fe}_2\text{O}_3$ is cubic and differs from magnetite in that cation vacancies exist in the structure. It is known that under certain conditions magnetite oxidizes to $\gamma\text{Fe}_2\text{O}_3$ followed by transformation to $\alpha\text{Fe}_2\text{O}_3$. Due to the similarity in crystal structure between $\gamma\text{Fe}_2\text{O}_3$ and magnetite, direct evidence for the transformation has been difficult to obtain, and the subject remains controversial.

Kojima⁴ studied the transformations in iron oxides by following the magnetic remanence and coercive force as a function of temperature in various atmospheres. He concluded that $\gamma\text{Fe}_2\text{O}_3$ is an intermediate product in both the oxidation of magnetite to $\alpha\text{Fe}_2\text{O}_3$ and in the reduction of $\alpha\text{Fe}_2\text{O}_3$ to magnetite. David and Welch⁵ investigated magnetite prepared by reduction of $\alpha\text{Fe}_2\text{O}_3$ and by precipitation. Only the magnetite prepared by precipitation showed the formation of $\gamma\text{Fe}_2\text{O}_3$ on oxidation. The authors concluded that $\gamma\text{Fe}_2\text{O}_3$ is stable only if water is present in the lattice. Behar⁶ conducted a micrographic study of

the oxidation of magnetite, and concluded that oxidation occurs first in the [111] direction.

The oxidation of magnetite has been investigated by differential thermal analysis by several investigators. Magnetite shows two characteristic exothermic peaks. The first peak occurs at about 300°C, while the second broader peak occurs at about 900°C. Kulp and Trite⁷ concluded that synthetic magnetite, prepared by a reduction of $\alpha\text{Fe}_2\text{O}_3$ at low temperatures, is transformed to $\gamma\text{Fe}_2\text{O}_3$, but they attributed the first peak in natural magnetite to recrystallization with no formation of $\gamma\text{Fe}_2\text{O}_3$ occurring. This conclusion is based on the facts that the size of the peak is proportional to particle size, and that the material heated beyond the first peak contains a considerable amount of ferrous iron. Schmidt and Vermaas⁸ concluded that the first peak in natural magnetite is due to surface oxidation and the second peak to volume oxidation instigated by recrystallization of the protective surface layer of $\alpha\text{Fe}_2\text{O}_3$. They agree with Kulp and Trite, that no $\gamma\text{Fe}_2\text{O}_3$ is formed.

An investigation of the oxidation of the solid-solution series $\text{Ni}_{.474}\text{Zn}_{.526}\text{Fe}_2\text{O}_4 - \text{Fe}_3\text{O}_4$ has been undertaken to attempt to understand the processes involved in oxidizing the ferrous iron in solid solution with the nickel-zinc ferrosphenel. The samples used were prepared by ball-milling NiO , ZnO , and $\alpha\text{Fe}_2\text{O}_3$ in acetone for six hours. The oxides were dried, pressed into compacts, fired in air for 1425°C for one hour, and water-quenched. The samples were then crushed and passed through a 325-mesh sieve. The differential thermal analysis curves were obtained with a unit built according to the Department of Agriculture design. A platinum-vs-platinum-10%-rhodium differential thermocouple was used at a sensitivity setting of 2.9 microvolts per centimeter. A chromel-alumel thermocouple was used to determine the temperature of the block. This thermocouple was calibrated against the inversion temperature of quartz using the procedure given by Faust.⁹ The heating rate was 12°C per minute.

The differential thermal curves are shown in Fig. 1. The curves show a slight exothermic peak at 360°C from the Curie temperature of the nickel sample holder. The curve for magnetite shows the two characteristic exothermic peaks along with a break at the Curie temperature of magnetite, 585°C. To identify the cause of the exothermic peaks, the oxidation of magnetite was followed by determining the change in weight, and the change in ferrous iron content of a sample heated in air for 15 minutes at 50°C temperature intervals. Figure 2 shows the percent change in weight. There is a break in the curve between 250° and 300°C. This same break was obtained in the ferrous iron content of the samples. The change in rate of oxidation at this temperature interval would appear to explain the low-temperature exothermic peak in the differential thermal curve of magnetite. It is concluded that this peak in magnetite is caused by surface oxidation, as proposed by Schmidt and Vermaas.⁸

Schmidt and Vermaas state that the oxidation of magnetite is accelerated at the Curie temperature. Figure 2 shows no indication that this is the case. It appears that the second peak is not due to any sudden initiation of oxidation

but rather makes its appearance when the continuously increasing rate of oxidation becomes sufficiently rapid.

Curves 1 through 9 of Fig. 1 are the differential thermal curves for the solid-solution series $\text{Ni}_{.474}\text{Zn}_{.526}\text{Fe}_2\text{O}_4 - \text{Fe}_3\text{O}_4$. Curve 1 shows a broad exothermic peak, due to the oxidation of the ferrous iron formed in the stoichiometric ferrosphenel at the temperature of formation of 1425°C . As the magnetite content is increased in Curves 2 to 9, this peak becomes less broad and moves down in temperature and corresponds with the low temperature peak in magnetite. Curves 8 and 9 have what appears to be two superimposed peaks. There is the possibility that the first of these two peaks increases in amplitude to become the low-temperature peak in magnetite. This does not seem as likely as the above explanation. In Curve 4 a second exothermic peak makes its appearance. This peak moves down in temperature with increasing magnetite content and decreases in amplitude, until it has almost disappeared in Curve 10. A third higher temperature peak makes its appearance in Curve 6. (The second peak in Curve 5 might well be a summation of two superimposed peaks.) This third peak moves up in temperature and corresponds with the high-temperature peak in the magnetite curve.

By identifying the exothermic peaks in the solid-solution series with those in magnetite, it can be concluded that the surface oxidation of the magnetite in solid solution occurs at a higher temperature than in magnetite itself, and the oxidation in the interior occurs at a lower temperature. The peak occurring at the intermediate temperature is thought to be due to the transformation of $\gamma\text{Fe}_2\text{O}_3$ to $\alpha\text{Fe}_2\text{O}_3$. Since Michel and Lensen¹⁰ and others have shown that certain foreign ions stabilize the $\gamma\text{Fe}_2\text{O}_3$ structure, it seems reasonable to assume that in the solid solutions investigated some stabilization of $\gamma\text{Fe}_2\text{O}_3$ has occurred.

THE SOLID-STATE REACTION

The use of differential thermal analysis to study the formation of the ferrosphenel from the oxides was attempted. The sintering of the material to the thermocouple proved to be a problem, and only one or two runs were possible before it became necessary to replace the differential thermocouple.

The differential thermal curves of Fig. 3 were obtained from oxide samples ball-milled to insure proper mixing. The equipment used was similar in design to that described above, but the recording was made with an X-Y Recorder. The sensitivity was 200 microvolts per cm and the heating rate was 25° per minute. A stainless steel sample holder replaced the nickel one.

All the curves in Fig. 3 show an exothermic peak between 300 and 325°C . Curve 1 is from magnetite prepared by firing $\alpha\text{Fe}_2\text{O}_3$ at 1425°C while Curve 2 is from $\alpha\text{Fe}_2\text{O}_3$ ball-milled for six hours in acetone. Curve 3 is from the same

$\alpha\text{Fe}_2\text{O}_3$ before it was ball-milled. From the resemblance between the low-temperature peaks in Curves 1 and 2, it is concluded that a surface layer of magnetite is formed on the $\alpha\text{Fe}_2\text{O}_3$ particles.

Curves 4 through 8 are for the following oxide mixtures: $\text{NiO} + \text{Fe}_2\text{O}_3$; $\text{ZnO} + \text{Fe}_2\text{O}_3$; $.4 \text{ NiO} + .6 \text{ ZnO} + \text{Fe}_2\text{O}_3$; $.474 \text{ NiO} + .526 \text{ ZnO} + 1.294 \text{ Fe}_2\text{O}_3$; and $.4 \text{ NiO} + .6 \text{ ZnO} + \text{Fe}_2\text{O}_3 + .0075 \text{ V}_2\text{O}_5$, respectively. The break at 680° in Curves 2 through 8 corresponds to the temperature of transformation of $\alpha\text{Fe}_2\text{O}_3$ from an antiferromagnetic state to a paramagnetic state. According to Willis and Rooksky,¹¹ there is a sudden expansion along the triad axis and a change in the rhombohedral angle on cooling through this temperature. There is an indication that $\text{NiO} + \text{Fe}_2\text{O}_3$ (Curve 4) reacts at a higher temperature than $\text{ZnO} + \text{Fe}_2\text{O}_3$ (Curve 5). The curves for samples of $.4 \text{ NiO} + .6 \text{ ZnO} + \text{Fe}_2\text{O}_3$ and $.474 \text{ NiO} + .526 \text{ ZnO} + 1.294 \text{ Fe}_2\text{O}_3$ are difficult to interpret. Curve 6 resembles Curve 5, while Curve 7 appears to have a double peak at the higher temperatures. The addition of V_2O_5 in small amounts has been shown by Grimes, Thomassen, Jefferson, and Kothary¹² to lower the temperature of ferrosphenel formation. Curve 8 from material containing a small amount of V_2O_5 shows a decided exothermic peak at about 820°C . It is interesting to note that the melting point of V_2O_5 is given as 800°C in the Handbook of Chemistry.¹³

CONCLUSION

The oxidation of magnetite occurs in two stages. The surface oxidation at about $250\text{-}300^\circ\text{C}$ is marked by a sharp exothermic peak in the differential thermal curve. The rate of volume oxidation increases with temperature and becomes sufficiently rapid at the higher temperatures to give rise to a second broad exothermic peak at 900°C . The surface oxidation of magnetite in solid solution with a nickel-zinc ferrosphenel occurs at a higher temperature than in magnetite itself, while the volume oxidation occurs at a lower temperature. A third exothermic peak occurs in the intermediate compositions which has tentatively been identified with the transformation of $\gamma\text{Fe}_2\text{O}_3$ to $\alpha\text{Fe}_2\text{O}_3$.

The use of differential thermal analysis to study the solid-state reaction occurring during the formation of the ferrosphenel from the oxides did not prove very informative. There is an indication that $\text{NiO} + \text{Fe}_2\text{O}_3$ reacts at a higher temperature than does $\text{ZnO} + \text{Fe}_2\text{O}_3$. The presence of an exothermic peak in all material ball-milled in steel ball mills was traced to $\alpha\text{Fe}_2\text{O}_3$. The similarity in the differential thermal peak of this material to that of magnetite leads to the conclusion that magnetite has formed on the surface of the particles. The addition of small amounts of V_2O_5 to the oxide mixture is known to lower the ferrosphenel formation. Differential thermal curves of the material shows an exothermic peak near the melting point of V_2O_5 .

REFERENCES

1. C. F. Jefferson, An Investigation of the Composition on an Iron-Rich Nickel-Zinc Ferrite. Technical Report No. 66, Electronic Defense Group, Department of Electrical Engineering, The University of Michigan, June, 1956.
2. C. F. Jefferson, and D. M. Grimes, A Study of the Preparation of Nickel-Zinc Ferrites, Technical Report No. 58, Electronic Defense Group, Department of Electrical Engineering, The University of Michigan, January, 1956.
3. L. G. Van Uitert, "dc Resistivity in the Nickel and Nickel-Zinc Ferrite System," J. of Chem. Physics, 23, 1883-1887 (1955).
4. H. Kojima, On the Magnetic Property of Iron Oxides, The Science Reports of the Research Institutes, Tohoku University, Series A 6, 178-183 (1954).
5. I. David, and A. J. E. Welch, "The Oxidation of Magnetite and Related Spinels," Trans. of the Faraday Society, 52, 1642-50 (1956).
6. I. Behar, "Micrographic Study of the Oxidation of Magnetite," Comptes Rendus, 243, 1877-1880 (Dec., 1956).
7. S. L. Kulp, and A. F. Trite, "Differential Thermal Analysis of Natural Ferric Oxide," American Mineralogist, 36, 23-44 (1951).
8. E. R. Schmidt, and F. H. S. Vermaas, "Differential Thermal Analysis and Cell Dimensions of Some Natural Magnetites," American Mineralogist, 40, 422-431 (1955).
9. G. T. Faust, "Thermal Analysis of Quartz and Its Use in Calibration of Thermal Studies," American Mineralogist, 33, 337-345 (1948).
10. A. Michel, and M. Lensen, "On the Stabilization of the Cubic Sesquioxide of Iron," Comptes Rendus, 243, 1422-1423 (1956).
11. B. T. M. Willis, and H. P. Rooksky, "Crystal Structure and Antiferromagnetism on Haematite," Phys. Society of London, B, 65, 950-954 (1952).
12. D. M. Grimes, L. Thomassen, C. F. Jefferson, and N. C. Kothary, "Effect of V₂O₅ on Nickel-Zinc Ferrite Formation," J. Chem. Phys., 23, 2205, 1955.
13. Handbook of Chemistry, Ed. N. A. Lange, Handbook Pub., Inc., Sandusky, 1944.

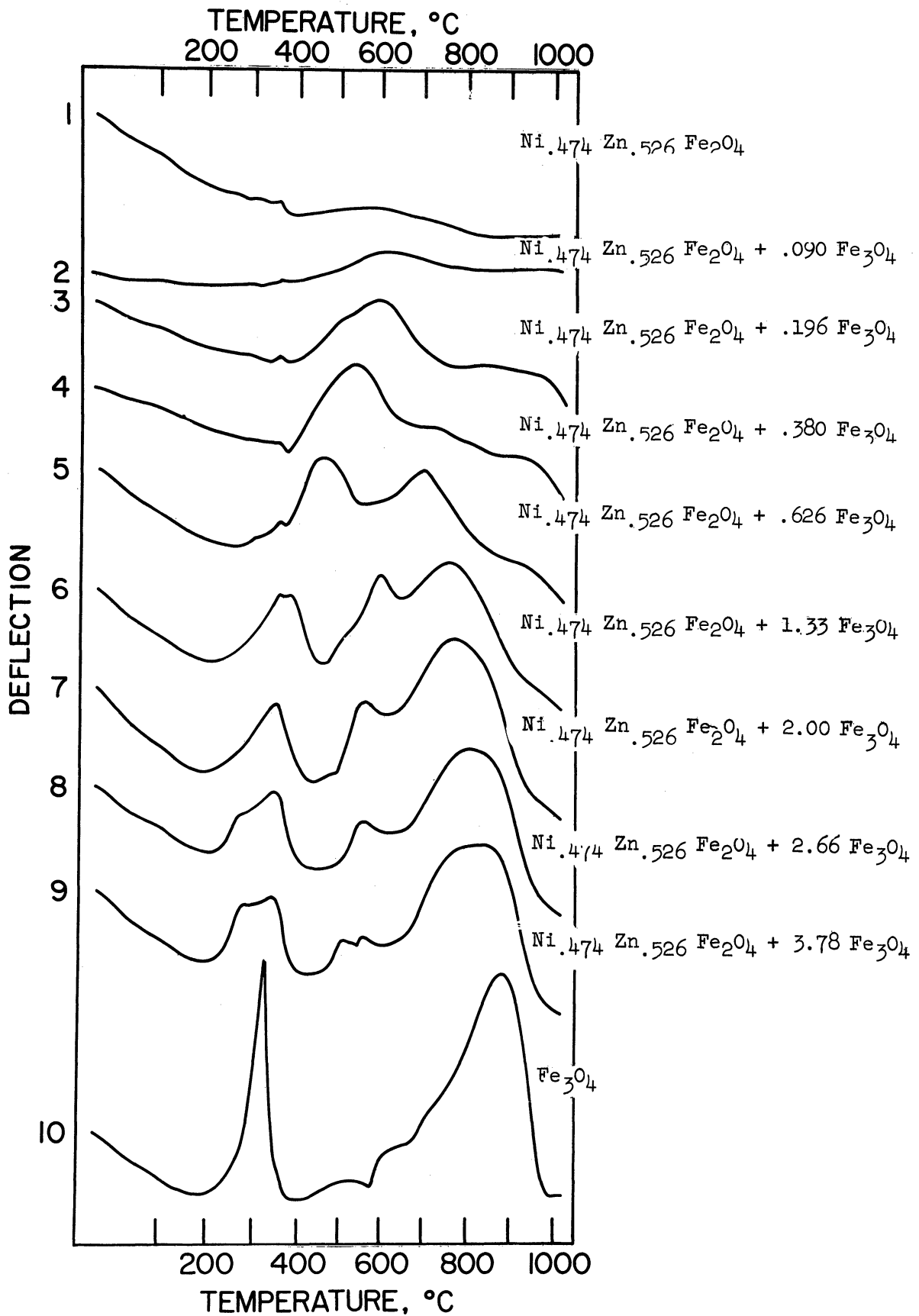


Fig. 1. Differential thermal curves for the solid solution series Ni_{0.474}Zn_{0.526}Fe₂O₄ - Fe₃O₄.

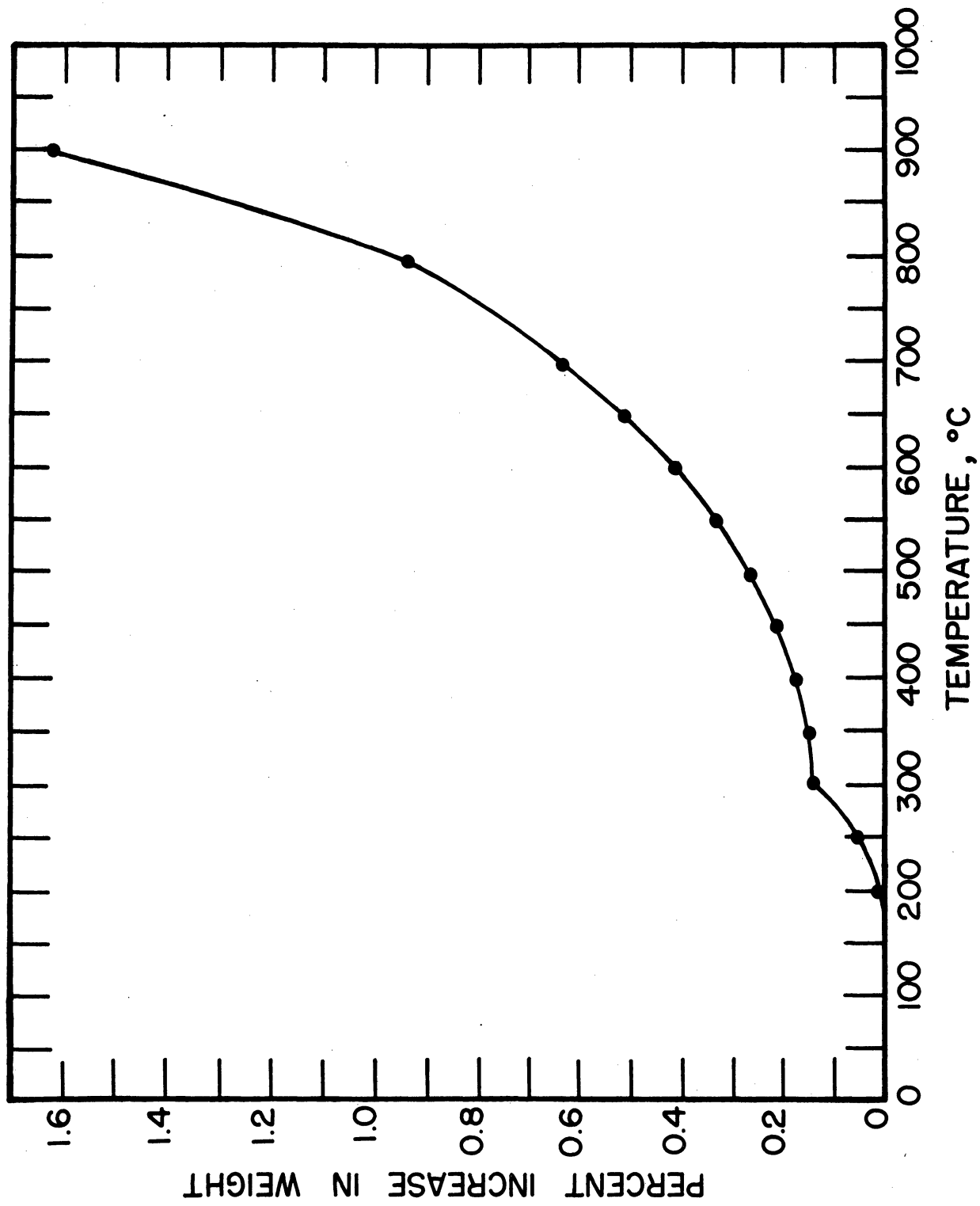


Fig. 2. Change in weight of magnetite as a function of oxidation temperature; heating time 15 minutes.

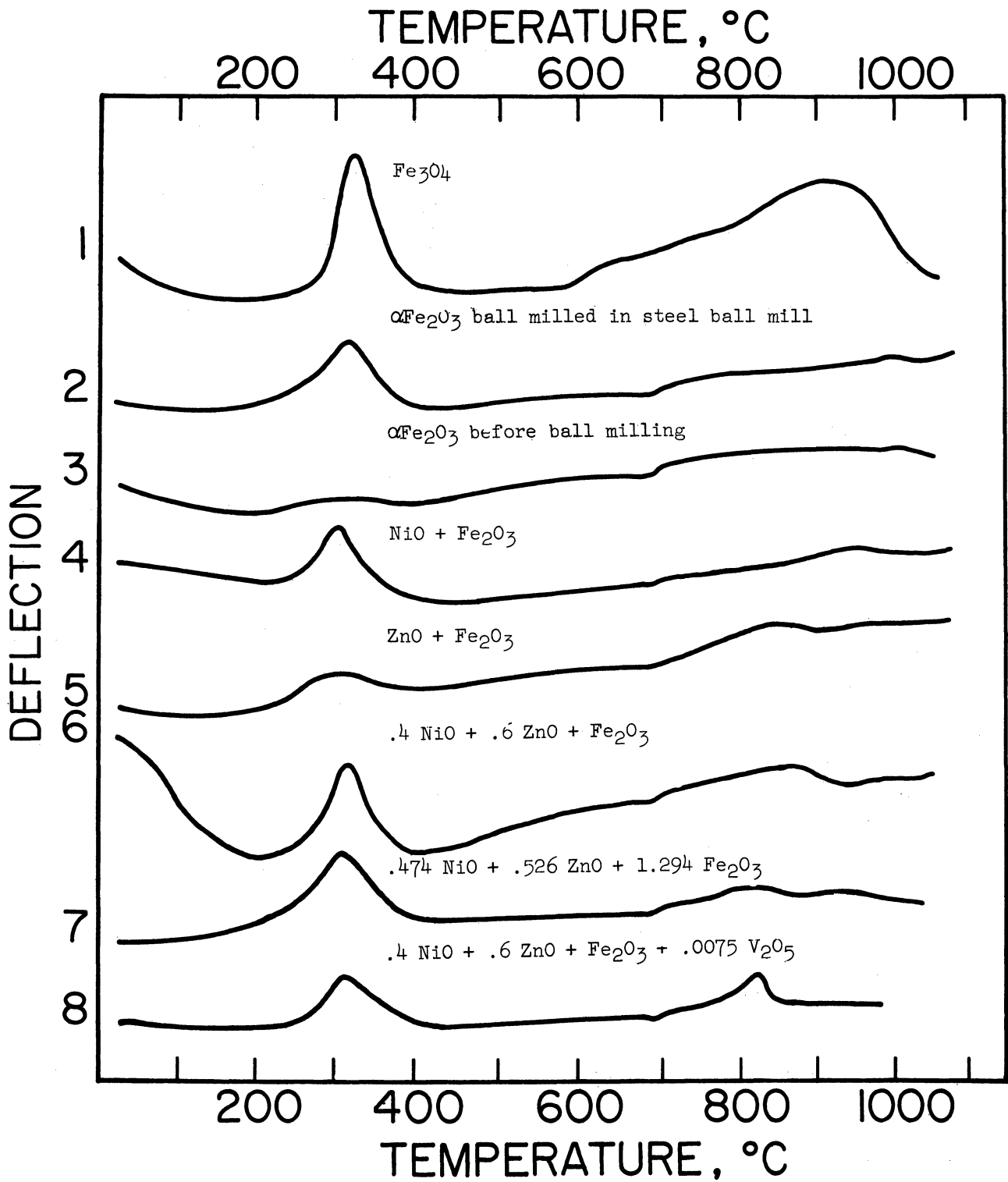


Fig. 3. Differential thermal curves of the formation of the ferrosipinel from the oxides.

DISTRIBUTION LIST

<u>Agency</u>	<u>No. of Copies</u>	<u>Agency</u>	<u>No. of Copies</u>
Commander Hq., AF Office of Scientific Research, ARDC Attn: SRQB Washington 25, D. C.	5	Director of Research and Development Hq., U. S. Air Force Attn: AFDRD-RE-3 Washington 25, D. C.	1
Commander Wright Air Development Center Attn: WCRRH Attn: WCRRL Attn: WCRTL Attn: WCRIM-1 Wright-Patterson Air Force Base, Ohio	4	Department of the Navy Office of Naval Research Attn: Code 423 Attn: Code 421 Washington 25, D. C.	2
Commander Air Force Cambridge Research Center Attn: Technical Library Attn: CRRF L. G. Hanscom Field Bedford, Massachusetts	2	Officer-in-Charge Office of Naval Research Navy No. 100 Fleet Post Office New York, New York	1
Commander Rome Air Development Center Attn: Technical Library Griffiss Air Force Base Rome, New York	1	Commanding Officer Naval Radiological Defense Laboratory San Francisco Naval Shipyard San Francisco 24, California	1
Director, Office for Advanced Studies Air Force Office of Scientific Research P. O. Box 2035 Pasadena 2, California	1	Director, Research and Develop- ment Division, General Staff Department of the Army Washington 25, D. C.	1
Document Service Center Armed Services Technical Information Agency Knott Building Dayton 2, Ohio	10	Division of Research U. S. Atomic Energy Commission 1901 Constitution Avenue, N.W. Washington 25, D. C.	1
		U. S. Atomic Energy Commission Library Branch Technical Information Division, ORE P. O. Box E Oak Ridge, Tennessee	1

The University of Michigan • Engineering Research Institute

DISTRIBUTION LIST (concluded)

<u>Agency</u>	<u>No. of Copies</u>	<u>Agency</u>	<u>No. of Copies</u>
Oak Ridge National Laboratory Attn: Central Files P. O. Box P Oak Ridge, Tennessee	1	Commander Western Development Division (ARDC) Attn: WDSIT, P. O. Box 262 Inglewood, California	1
Brookhaven National Laboratory Attn: Research Library Upton, Long Island, New York	1	Document Custodian Los Alamos Scientific Laboratory P. O. Box 1663 Los Alamos, New Mexico	1
Argonne National Laboratory Attn: Librarian P. O. Box 299 Lemont, Illinois	1	Arnold Engineering Development Center, Attn: Tech. Library P. O. Box 162 Tullahoma, Tennessee	1
Ames Laboratory Iowa State College P. O. Box 14A, Station A Ames, Iowa	1	Commanding Officer Ordnance Materials Research Office Watertown Arsenal Watertown 72, Massachusetts	1
Knolls Atomic Power Laboratory Attn: Document Librarian P. O. Box 1072 Schenectady, New York	1	Commanding Officer Watertown Arsenal Watertown 72, Massachusetts Attn: Watertown Arsenal Labs. Tech. Reports Section	1
National Bureau of Standards Library, Room 203 Northwest Building Washington 25, D. C.	1	Commander, Hq., AF Office of Scientific Research, ARDC Attn: SREC, Tech. Library Washington 25, D. C.	2
National Science Foundation 1520 H. Street, N.W. Washington 25, D. C.	1	Commander, WADC Air Technical Intelligence Center Attn: Deputy for Documentation WPAFB, Ohio	1
Director, Office of Ordnance Research, Box CM, Duke Station Durham, North Carolina	1	(Inner envelope—no postage) Commander, European Office c/o American Embassy, ARDC Brussels, Belgium	1
Office of Technical Services Department of Commerce Washington 25, D. C.	1	(Outer envelope—postage) Superintendent, Diplomatic Pouch Rooms, Department of State Washington 25, D. C.	
NACA 1512 H. Street, N.W. Washington 25, D. C.	1		

UNIVERSITY OF MICHIGAN



3 9015 03025 4984